(2)

GENCORP
AEROJET

The Multiple Scattering Contributions In The Strong Fluctuation Theory To The Microwave Brightness Temperature

February 1994
Report No. 9617

Contract No. N00014-91-C-0140

by
Alex Stogryn and Mostafa A. Karam

Prepared for

OFFICE OF NAVAL RESEARCH
DEPARTMENT OF THE NAVY
Arlington, Virginia 22217

Prepared by

Aerojet Electronic Systems Plant
1100 West Hollyvale Street
Azusa, California 91702

Aerojet

THE MULTIPLE SCATTERING CONTRIBUTIONS IN THE STRONG FLUCTUATION THEORY TO THE MICROWAVE BRIGHTNESS TEMPERATURE

February 1994

Report No. 9617

Contract No. N00014-91-C-0140

Accesion For		
NTIS CRA&I	☑	
DTIC TAB	☐	
Unannounced	☐	
Justification		
By Dr. C. Luther		
Distribution / ONR/Code 1121RS		
Availability Codes 4/6/96		
Dist	Avail and/or Special	
A-1		

by

Alex Stogryn and Mostafa A. Karam

Prepared for

OFFICE OF NAVAL RESEARCH
DEPARTMENT OF THE NAVY
Arlington, Virginia 22217

Prepared by

Aerojet Electronic Systems Plant
1100 West Hollyvale Street
Azusa, California 91702

LIST OF FIGURES

I. INTRODUCTION

This study is a sequel to earlier studies [1-2] performed at Aerojet Electronic Systems Plant under a previous contract with the Office of Naval Research to account for the contribution of multiple scattering to microwave brightness temperature of sea ice and its snow cover. The application of the distorted Born approximation in conjunction with the strong fluctuation theory has led to calculated values for brightness temperatures in agreement with measurements from sea ice and its snow cover at frequencies below 37 GHz [3-4]. However, at frequencies above 37 GHz, the distorted Born approximation overestimates the brightness temperature. This is due to the fact that the distorted Born approximation accounts only for the singly scattered field. Physical and mathematical arguments given in [1-2] showed that inclusion of higher order multiple scattering would lead to more reasonable values for the brightness temperature at higher frequencies where the multiple scattering is expected to be dominant.

An extension of the distorted Born approximation was carried out [1] to include higher order multiple scattering. Strong fluctuation theory was employed to derive a set of integral equations describing the second moment of the multiply scattered field for a multi-layered anisotropic medium with planer interfaces. Various numerical considerations and the programming of these equations on a digital computer to obtain numerical results were left to a further study.

The present study addresses those numerical problems and describes results obtained from a computer program written to calculate brightness temperature of snow over ground. To calculate emissivities based on the equations in [1], a number of five-fold integrals (three to calculate second moments of the electric field and two to calculate the bi-static cross sections from these second moments) needed to be evaluated in addition to solving a coupled set of integral equations. This is clearly a large numerical problem requiring extensive computer

resources. Fortunately, it was found possible to perform two of these integrals analytically, thus reducing the problem to three-fold integrations and reducing the computational burden considerably. In addition, maximum use was made of symmetries in the kernels in order to simplify the integral equations to be solved.

To meet the objective of this study, Peake's formula is used in Sec.II to relate the brightness temperatures to the bi-static cross sections associated with the multiply scattered field. Then the symmetry characteristics of the medium are employed to simplify the relation between the bi-static cross sections and the field second moment. The integral equations describing the field second moment are stated in Sec.III. The equations contain kernels with triple integrals. One integral is over the medium depth. The second integral is over the spectrum of the azimuthal wave number, and the third is over the difference between the heights of the Green's function source points. Analytic evaluation for the integral over the higher part of the azimuth wave number spectrum is performed. Also, the integral over the difference between the heights of Green's function source point is carried out analytically. The integrals over the lower part of the wave number spectrum and over the medium depth are carried out numerically.

In Sec.IV, the procedures applied to solve the integral equations are described and some limitations of those procedures are pointed out. Finally in Sec.V, numerical results for snow over a soil surface, illustrating the behavior of the brightness temperature as function of medium depth for different radiometer frequencies and polarizations, are given. Those results are compared with corresponding calculations obtained via the distorted Born approximation .

In addition to the work explicitly contained in this report, the contract called for a critical review of chapters in a planned monograph on sea ice (subsequently published in 1992 by the American Geophysical Union as " Microwave Remote Sensing of Sea Ice", edited by F. Carsey). Two separate reviews, one for the preliminary draft of Chapter 10 (dealing with theory) and one

reviewing the preliminary draft of the monograph as a whole, were written and provided to the editor during the course of preparation of the monograph. A discussion of this work is not included here.

II. THE BRIGHTNESS TEMPERATURE ASSOCIATED WITH MULTIPLE SCATTERING

The geometry of the problem under consideration is shown in Fig.1, where the snowpack is treated as an isotropic multi-layered medium with plane interfaces over a homogeneous half space. The homogeneous half space stands for the ground. Since there is no adequate information about the physical temperature profile within the snowpack, the latter is assumed to be isothermal. Under this restriction the medium emissivity can be related to the random field bi-static cross sections through Peake's formula [3];

$$e_a(\bar{k}_o) = 1 - \left|Ra(\bar{k}_o)\right|^2 - \frac{1}{4\pi}\iint \sin\theta \, d\theta \, d\phi \left\{\gamma_{ah}(\bar{k}_o,\bar{k}) + \gamma_{ah}(\bar{k}_o,\bar{k})\right\} \tag{1}$$

where $\bar{k}_o$ (θo, ϕo) is the observation direction, a ($a = v, h$) is the sensor polarization, $R_a(\bar{k}_o)$ is the reflection coefficient, and $\gamma_{aq}(\bar{k}_o,\bar{k})$, ($q = v, h$) is the bi-static cross section of the random field in the $\bar{k}_o$ direction with polarization a due to a plane wave propagating in $\bar{k}\,(\theta, \phi)$ direction exciting the medium. To examine the contribution of the multiple scattering to the brightness temperature we write the random field as

$$\bar{E}_{ra} = \bar{E}_{rs} + \bar{E}_{rm} \tag{2}$$

where $\bar{E}_{rs}$ is the random field due to single scattering (distorted Born approximation), and $\bar{E}_{rm}$ is the random field due to multiple scattering. Since the bi-static cross sections are proportional to the intensity of the scattered random field from (2) we obtain,

$$< |\bar{E}_r.\hat{a}|^2 > = < |\bar{E}_{rs}.\hat{a}|^2 > + < |\bar{E}_{rm}.\hat{a}|^2 > \tag{3}$$

Accordingly the bi-static cross section can be written as

$$\gamma_{aq}(\bar{k}_O,\bar{k}) = \gamma^s_{aq}(\bar{k}_O,\bar{k}) + \gamma^l_{aq}(\bar{k}_O,\bar{k}) \tag{4}$$

The first term in (4) stands for the bi-static cross section obtained via distorted Born approximation (single scattering). The second term is the bi-static cross section associated with the higher orders of multiple scattering. By substituting (4) into (1) the emissivity is reduced to

$$e_a(\bar{k}_O) = e^S_a(\bar{k}_O) - \frac{1}{4\pi}\iint \sin\theta d\theta d\phi \left\{\gamma^l_{ah}(\bar{k}_O,\bar{k}) + \gamma^l_{av}(\bar{k}_O,\bar{k})\right\} \tag{5}$$

where ,

$$e^s_a(\bar{k}_o) = 1 - |R_a(\bar{k}_o)|^2 - \frac{1}{4\pi}\iint \sin\theta d\theta\, d\phi\, \{ \gamma^s_{ah}(\bar{k}_o,\bar{k}) + \gamma^s_{ah}(\bar{k}_o,\bar{k}) \} \tag{6}$$

is the emissivity obtained via the distorted Born approximation (single scattering).

Then by adding the effect of the earth atmosphere to (5), the brightness temperature of the radiation leaving the earth surface at $z = 0$ in direction $\bar{k}_o$ with polarization "a" is

$$T_a(\bar{k}_o) = T^S_a(\bar{k}_o) - T^l_a(\bar{k}_o) \tag{7}$$

where $T_a^s(\bar{k}_o)$ is the brightness temperature obtained via distorted Born approximation (single scattering),

$$T_a^S(\bar{k}_o) = e_a^S(\bar{k}_o)T_g + |R_a(\bar{k}_O)|^2 T_{sky}(\bar{k}_o) + \frac{1}{4\pi}\iint \left\{ \gamma_{ah}^S(\bar{k}_o,\bar{k}) + \gamma_{ah}^S(\bar{k}_o,\bar{k}) \right\} T_{sky}(\bar{k}) \sin\theta d\theta d\phi \tag{8}$$

and $T_a^I(\bar{k}_o)$ is the multiple scattering contribution to the brightness temperature,

$$T_a^I(\bar{k}_o) = \frac{1}{4\pi}\iint \{\gamma_{ah}^I(\bar{k}_o,\bar{k}) + \gamma_{av}^I(\bar{k}_o,\bar{k})\}\{T_g - T_{sky}(\bar{k})\} \sin\theta d\theta d\phi \tag{9}$$

In (8) and (9) T_g is the ground physical temperature and $T_{sky}(\bar{k}_o)$ is the brightness temperature of sky radiation. In this study the ground physical temperatures is taken to be independent on θ and ϕ. The sky temperature is assumed to be a function of θ only.

As we can see from (9), the contribution of multiple scattering to the brightness temperature depends mainly on the difference between the ground and sky temperatures. At microwave frequencies, the ground physical temperature is higher than the sky brightness temperature. Accordingly, the higher order multiply scattered field tends to reduce the brightness temperature. The reduction is proportional to the bi-static cross sections associated with the multiply scattered field.

Eq. (7) gives the brightness temperature at the earth surface. When this radiation is propagated through the atmosphere, it undergoes some modifications due to the atmospheric attenuation and emission. These effects can be accounted for following the same procedures reported in [2].

In (10), the bi-static cross sections are related the field second moment through the relation [1];

$$\gamma^{I}_{eq}(\bar{k}_o,\bar{k}) = [k_o^2\cos\theta/(\pi\cos\theta_o)]\; b_i b_j \int_{-\infty}^{0} dz' \int_{-\infty}^{0} dz''\; A_{ik}(z',k_x,k_y)$$
$$A^{*}_{jt}(z'',k_x,k_y)\, F_{kta}(k_x,k_y,z',z'') \tag{10}$$

where symbol * denotes complex conjugate, the $F_{kta}(k_x,k_y,z',z'')$ is the kt element of the two dimensional Fourier transform

$$\overline{\overline{F}}_a(k_x,k_y,z',z'') = \int_{-\infty}^{\infty} dxdy\, C(|r'-r''|)\exp(i k_x x + i k_y y) < \overline{E}_{ra}(\bar{r}')\overline{E}^{*}_{ra}(\bar{r}'') >$$

$$C(|r'-r''|) = <\xi(r')\,\xi^{*}(r'')>$$

$$\xi(r') = \Delta L / [1 + S\,\Delta L]$$

$$\Delta L = k_o^2(K_o - K^r)$$

$$S = -1/(3k_o^2 K_o) \tag{11}$$

Here K_o is the quasi-static dielectric constant, K^r [5] is random dielectric constant of the medium, S is the coefficient of the delta function part of the Green's function and $C(|\bar{r}'-\bar{r}''|)$ is the correlation function.

In (10), $A_{ik}(z',k_x,k_y)$ is the ik element of the two dimensional Fourier transform of the dyadic Green's function $\overline{\overline{\Gamma}}(\bar{r},\bar{r}')$ with

$$\overline{\overline{\Gamma}}(r,r') = (2\pi)^{-2} \int_{-\infty}^{\infty} dk_x \int_{-\infty}^{\infty} dk_y\, \overline{\overline{A}}(z',k_x,k_y) \exp\{i[k_x(x-x') + k_y(y-y') + k_z z]\}$$

(12)

and

$$k_x^2 + k_y^2 + k_z^2 = k_o^2$$

$$\overline{\overline{A}}(z',k_x,k_y) = A_{\rho\rho}(z',\theta)\,\hat{\rho}\hat{\rho} + A_{\rho z}(z',\theta)\,\hat{\rho}\hat{z} + A_{\phi\phi}(z',\theta)\,\hat{\phi}\hat{\phi} + A_{z\rho}(z',\theta)\,\hat{z}\hat{\rho} + A_{zz}(z',\theta)\,\hat{z}\hat{z}$$

(13)

In (13), $\hat{\rho}$, $\hat{\phi}$, and $\hat{z}$ are unit vectors along the cylindrical coordinates, and

$$k_x^2 + k_y^2 = \rho^2, \qquad \rho = k_o \sin\theta$$

(14)

Due to the medium symmetry around z axis, (x,y), (y,x), and (z,y) components of the field second moment dyad vanish. Thus as shown in [1],

$$\gamma^I_{ah}(\bar{k}_o,\bar{k}) = (k_o\cos\theta)^2 / (\pi\cos\theta_o) \int_{-\infty}^{\infty} dz' \int_{-\infty}^{\infty} dz''\, A_{\phi\phi}(z',\theta) A^*_{\phi\phi}(z'',\theta)\,.$$
$$[\sin^2\phi\, F_{11a}(z',z'') + \cos^2\phi\, F_{22a}(z',z'')]$$

(15)

$$\gamma^I_{av}(\bar{k}_o,\bar{k}) = k_o^2 / (\pi\cos\theta_o) \int_{-\infty}^{\infty} dz' \int_{-\infty}^{\infty} dz''\, \{A_{\rho\rho}(z',\theta)\, A^*_{\rho\rho}(z',\theta)\,.\,[\cos^2\phi\, F_{11a}(z',\theta)$$
$$+ \sin^2\phi\, F_{22a}(z',z'')] + \cos\phi\,[A_{\rho\rho}(z',\theta)\;\; A^*_{\rho z}(z'',\theta)\, F_{13a}(z',z'')$$
$$+ A_{\rho z}(z',\theta)\, A^*_{\rho\rho}(z'',\theta)\, F_{31a}(z',z'')] + A_{\rho z}(z',\theta)\, A^*_{\rho z}(z'',\theta)\, F_{33a}(z',z'')\}$$

(16)

Then by substituting (15) and (16) into (9) and performing the integration over $d\phi$, the contribution of the multiply scattered field to the brightness temperature can be written as

$$T_a^I(\bar{k}_o) = k_o^2 / (8\pi \cos\theta_o) \int_0^{\pi/2} \sin\theta d\theta \int_{-\infty}^{0} dz' \int_{-\infty}^{0} dz'' \{ [F_{11a}(z',z'') + F_{22a}(z',z'')] .$$

$$[\cos^2\theta \, A_{\phi\phi}(z',\theta) A^*_{\phi\phi}(z'',\theta) + A_{\rho\rho}(z',\theta) \, A^*_{\rho\rho}(z',\theta)] +$$

$$+ 2 \, A_{\rho z}(z',\theta) \, A^*_{\rho z}(z'',\theta) \, F_{33a}(z',z'') \} \{T_g - T_{sky}(k)\}$$

(17)

In (17), the F_{iia}'s (i = 1, 2, 3) are the diagonal elements of the $\overline{\overline{F}}_a(k_x,k_y,z',z'')$ tensor (Eq. 11) when the exciting field is polarized in "a" direction ($a = v, h$). More simplification for (17) can be achieved if the correlation function $C(|\bar{r}' - \bar{r}''|)$ is assumed to be sharply peaked. In this case the diagonal elements of the $\overline{\overline{F}}_a(k_x,k_y,z',z'')$ tensor reduce to

$$F_{iia}(z',z'') = \langle e_{iia}(z') \rangle W(z',z'',k_x,k_y)$$

$$\langle e_{iia}(z') \rangle = \langle E_{ia}(z') E^*_{ia}(z') \rangle$$

$$W(z',z'',k_x,k_y) = \int_{-\infty}^{\infty} dx dy \, C(|\bar{r}' - \bar{r}''|) \exp(i k_x x + i k_y y)$$

(18)

For an exponential correlation function with

$$C(|\bar{r}' - \bar{r}''|) = \langle |\xi|^2 \rangle \exp(-|\bar{r}' - \bar{r}''| / \ell)$$

(19)

the Fourier transform $W(z',z'',k_x,k_y)$ can be written as [1]

$$W'(z',z'',k_x,k_y) = <|\xi|^2> \frac{2\pi}{\ell} p^{-3}[1+p|z'-z''|]\exp(-p|z'-z''|)$$

(20)

where

$$p = \left[1+\ell^2(k_x^2+k_y^2)\right]^{1/2}/\ell$$

(21)

Substituting (20) into (18) then substituting the resultant in (17) with and letting $z' = z_1$ and $z'' = z_1 + u$ (see Appendix 2 in [3] for a discussion of this transformation), the multiple scattering contribution to the brightness temperature can be written as

$$T_e^1(\bar{k}_o) = k_o^2/(2\cos\theta_o)\int_0^{\pi/2}\sin\theta d\theta\int_{-\infty}^{0} dz_1 \operatorname{Re}\{[E_{11a}(z_1)+E_{22a}(z_1)][\cos^2\theta|A_{\phi\phi}(z_1)|^2 I_{\phi\phi}(z_1,\theta)$$
$$+|A_{\rho\rho}(z_1,\theta)|^2 I_{\rho\rho}(z_1,\theta)] + 2E_{33a}(z_1)|A_{\rho z}(z_1,\theta)|^2 I_{\rho\rho}(z_1,\theta)\}[T_g - T_{sky}(\bar{k})]$$

(22)

where Re is the real part operator, and

$$I_{\phi\phi}(z_1,\theta) = \frac{1}{2\pi}\int_{-\infty}^{0} du\, W'(|u|,k_x,k_y)\exp\left(-\int_{z_1+u}^{z_1}\alpha_-(z'',\theta)\,dz''\right)$$

$$I_{\rho\rho}(z_1,\theta) = \frac{1}{2\pi}\int_{-\infty}^{0} du\, W'(|u|,k_x,k_y)\exp\left(-\int_{z_1+u}^{z_1}\beta_-(z'',\theta)\,dz''\right)$$

(23)

Here the functions α_- and β_- are related to the Green's function and were discussed in Appendix A of [1]. For convenient reference, they are reviewed in Appendix A of this study.

Explicit expressions for α_- and β_- are derived in Appendix B. The analytic evaluation for the integrals in (23) is performed in Appendix C.

Eqs. (22) and (23) give the multiply scattered field contribution to the brightness temperature for an isothermal snowpack. As we can see from (23) the brightness temperature over the snowpack surface is related to the field second moments within the snowpack. In the following section the integral equations describing second moments of the multiple scattered field will be considered and its reduction to a form suitable for digital computer programming will be investigated.

III. INTEGRAL EQUATIONS FOR THE MULTIPLY SCATTERED FIELD SECOND MOMENT

In [1] two uncoupled sets of integral equations have been derived for the multiply scattered field second moments. One set describes the diagonal components of the field second moment tensor, and the other set describes the off diagonal terms. Since the brightness temperature for a linearly polarized signal depends only on the diagonal components (see Eq. 17), they are the only components that will be considered here. From [1], we can write the integral equation describing those components as

$$E_{11a}(z) = \int_{-\infty}^{0} dz_1 \{D_{11}(z,z_1)\langle e_{11a}(z_1)\rangle + D_{12}(z,z_1)\langle e_{22a}(z_1)\rangle + b_{\rho z}(z,z_1)\langle e_{33a}(z_1)\rangle$$

$$E_{22a}(z) = \int_{-\infty}^{0} dz_1 \{D_{12}(z,z_1)\langle e_{11a}(z_1)\rangle + D_{11}(z,z_1)\langle e_{22a}(z_1)\rangle + b_{\rho z}(z,z_1)\langle e_{33a}(z_1)\rangle$$

$$E_{33a}(z) = \int_{-\infty}^{0} dz_1 \{b_{z\rho}(z,z_1)\langle e_{11a}(z_1)\rangle + b_{z\rho}(z,z_1)\langle e_{22a}(z_1)\rangle + 2\,b_{zz}(z,z_1)\langle e_{33a}(z_1)\rangle$$

$$\langle e_{iia}(z_1)\rangle = E_{iia}(z_1) + E^{c}_{iia}(z_1), \qquad i = 1,2,3 \tag{24}$$

where E^{c}_{iia} are the second moments of the coherent field when the exciting field is polarized in "*a*" direction, and

$$D_{11}(z,z_1) = 3/4\{b_{\rho\rho}(z,z_1) + b_{\phi\phi}(z,z_1) + 1/3\,b_{\rho\phi}(z,z_1)\}$$

$$D_{12}(z,z_1) = 1/4\{b_{\rho\rho}(z,z_1) + b_{\phi\phi}(z,z_1) - b_{\rho\phi}(z,z_1)\} \tag{25}$$

Here

$$b_{\alpha\beta}(z,z_1)=\frac{1}{2\pi}\,\mathrm{Re}\{\int_0^\infty \rho d\rho \int_{-\infty}^0 du\, W(|u|;z_1)\, a_{\alpha\beta}(z,z_1)\ \ a^*_{\alpha\beta}(z,z_1+u)\}$$

(26)

where the subscripts ($\alpha\beta$) are one of the pairs ($\rho\rho$), ($\phi\phi$), (ρz), or ($z\rho$). In (25),

$$b_{\rho\phi}(z,z_1)=\frac{1}{2\pi}\,\mathrm{Re}\{\int_0^\infty \rho d\rho \int_{-\infty}^0 du\, W(|u|;z_1)\,[a_{\rho\rho}(z,z_1)\ \ a^*_{\phi\phi}(z,z_1+u)+a_{\phi\phi}(z,z_1)\ \ a^*_{\rho\rho}(z,z_1+u)]\}$$

(27)

In (26) and (27) $a_{\alpha\beta}$'s are the components of the Green's function tensor with the snowpack which are given in Appendix A. Their relation to the Green's function elements in the upper half space (Eq. 13) is also given in Appendix A.

The problem of integrating over large values for the spectrum of azimuth wave number ρ can be overcome by writing the integral over ρ as

$$\int_0^\infty d\rho=\int_0^{\rho_1} d\rho+\int_{\rho_1}^\infty d\rho$$

(28)

where ρ_1 is a very large wave number. Then, by making use of the Green's function behavior for very large ρ, the second part of integration over ρ can be carried out analytically as shown in Appendix C of [1] reducing (24) to

$$E_{11a}(z)+m_1(z)\langle e_{11a}(z)\rangle+m_2(z)\langle e_{22a}(z)\rangle=\int_{-\infty}^0 d z_1\,\{M_{11}(z,z_1)\,\langle e_{11a}(z_1)\rangle+M_{12}(z,z_1)\,\langle e_{22a}(z_1)\rangle$$
$$+f_{\rho z}(z,z_1)\,\langle e_{33a}(z_1)\rangle\}$$

$$m_2(z)\langle e_{11a}(z)\rangle + E_{22a}(z) + m_1(z)\langle e_{22a}(z)\rangle = \int_{-\infty}^{0} dz_1 \{ M_{12}(z,z_1)\langle e_{11a}(z_1)\rangle + M_{11}(z,z_1)\langle e_{22a}(z_1)\rangle$$

$$+ f_{\rho z}(z,z_1)\langle e_{33a}(z_1)\rangle \}$$

$$E_{33a}(z) + m_3(z)\langle e_{33a}(z)\rangle = \int_{-\infty}^{0} dz_1 \{ f_{z\rho}(z,z_1)\langle e_{11a}(z_1)\rangle + f_{z\rho}(z,z_1)\langle e_{22a}(z_1)\rangle$$

$$+ M_{33}(z,z_1)\langle e_{33a}(z_1)\rangle \}$$

(29)

Explicit expressions for $m_1(z)$, $m_2(z)$, and $m_3(z)$ are given in [1]. In addition

$$M_{11}(z,z_1) = 3/4\{f_{\rho\rho}(z,z_1) + f_{\phi\phi}(z,z_1) - 1/3 f_{\rho\phi}(z,z_1)\}$$

$$M_{22}(z,z_1) = 1/4\{f_{\rho\rho}(z,z_1) + f_{\phi\phi}(z,z_1) - f_{\rho\phi}(z,z_1)\}$$

$$M_{33}(z,z_1) = 2 f_{zz}(z,z_1)$$

(30)

Here the subscripted functions f are identical to the subscripted functions b defined in (26) and (27) except for the fact that the upper limit of the integration over ρ is bounded by ρ_1 and the singularity is extracted from a_{zz}.

A further simplification for the integral equations can be achieved if the integration of the subscripted functions over u is evaluated. This can be achieved by using the translational property of the Green's function tensor elements (Appendix A) leading to;

$$f_{\phi\phi}(z,z_1) = \tfrac{1}{2\pi}\,\mathrm{Re}\{ \int_0^{\rho_1} \rho d\rho \int_{-\infty}^{0} du\, W'(|u|,z_1) \left| a_{\phi\phi}(z,z_1) \right|^2 \Im^*_{\phi\phi}(z_1,u) \}$$

$$f_{\rho\rho}(z,z_1) = \frac{1}{2\pi}\,\mathrm{Re}\{\int_0^{\rho_1}\rho d\rho \int_{-\infty}^{0} du\, W'(|u|,z_1)\,|\,a_{\rho\rho}(z,z_1)\,|^2\,\Im^*_{\rho\rho}(z_1,u)\}$$

$$f_{\rho z}(z,z_1) = \frac{1}{2\pi}\,\mathrm{Re}\{\int_0^{\rho_1}\rho d\rho \int_{-\infty}^{0} du\, W'(|u|,z_1)\,|\,a_{\rho z}(z,z_1)\,|^2\,\Im^*_{\rho\rho}(z_1,u)\}$$

$$f_{z\rho}(z,z_1) = \frac{1}{2\pi}\,\mathrm{Re}\{\int_0^{\rho_1}\rho d\rho \int_{-\infty}^{0} du\, W'(|u|,z_1)\,|\,a_{z\rho}(z,z_1)\,|^2\,\Im^*_{\rho\rho}(z_1,u)\}$$

$$f_{zz}(z,z_1) = \frac{1}{2\pi}\,\mathrm{Re}\{\int_0^{\rho_1}\rho d\rho \int_{-\infty}^{0} du\, W'(|u|,z_1)\,|\,a_{zz}(z,z_1)\,|^2\,\Im^*_{\rho\rho}(z_1,u)\}$$

$$f_{\rho\phi}(z,z_1) = \frac{1}{2\pi}\;\mathrm{Re}\int_0^{\rho_1} d\rho \int_{-\infty}^{0} du W'(|u|,z_1)\,\{\,a_{\rho\rho}(z,z_1)\,a^*_{\phi\phi}(z,z_1)\,\Im^*_{\phi\phi}(z,z_1)$$
$$+\,a_{\phi\phi}(z,z_1)a^*_{\rho\rho}(z,z_1)\,\Im^*_{\rho\rho}(z,z_1)\,\}$$

(31)

where

$$\Im_{\phi\phi}(z_1,u) = \exp[-\int_{z_1+u}^{z_1}\alpha_-(z'')dz''] \qquad \text{if } z > z_1+u$$
$$= \exp[\int_{z_1}^{z_1+u}\alpha_+(z'')\,dz''] \qquad \text{if } z < z_1+u$$

(32)

and

$$\Im_{\rho\rho}(z_1,u) = \exp[-\int_{z_1+u}^{z_1}\beta\_(z'')dz''] \qquad \text{if } z > z_1+u$$
$$= \exp[\int_{z_1}^{z_1+u}\beta_+(z'')dz''] \qquad \text{if } z < z_1+u$$

(33)

Then by carrying out the integral over u in (31) we obtain

$$f_{\phi\phi}(z,z_1) = \int_0^{\rho_1} \rho d\rho \left| a_{\phi\phi}(z,z_1) \right|^2 \ \mathrm{Re}\{ I_{\phi\phi}(z_1,\rho) \}$$

$$f_{\rho\rho}(z,z_1) = \int_0^{\rho_1} \rho d\rho \left| a_{\rho\rho}(z,z_1) \right|^2 \ \mathrm{Re}\{ I_{\rho\rho}(z_1,\rho) \}$$

$$f_{\rho z}(z,z_1) = \int_0^{\rho_1} \rho d\rho \left| a_{\rho z}(z,z_1) \right|^2 \ \mathrm{Re}\{ I_{\rho\rho}(z_1,\rho) \}$$

$$f_{z\rho}(z,z_1) = \int_0^{\rho_1} \rho d\rho \left| a_{z\rho}(z,z_1) \right|^2 \ \mathrm{Re}\{ I_{\rho\rho}(z_1,\rho) \}$$

$$f_{zz}(z,z_1) = \int_0^{\rho_1} \rho d\rho \left| a_{zz}(z,z_1) \right|^2 \ \mathrm{Re}\{ I_{\rho\rho}(z_1,\rho) \}$$

$$f_{\rho\phi}(z,z_1) = \int_0^{\rho_1} \rho d\rho \,\mathrm{Re}\{ a_{\rho\rho}(z,z_1) a^*_{\phi\phi}(z,z_1)\, I^*_{\phi\phi}(z_1,\rho) + a_{\phi\phi}(z,z_1) a^*_{\rho\rho}(z,z_1)\, I^*_{\rho\rho}(z_1,\rho)$$

(34)

where

$$I_{\phi\phi}(z_1,\rho) = \frac{1}{2\pi} \int_{-\infty}^{0} du\, W'(|u|, z_1)\, \Im_{\phi\phi}(z_1,\rho)$$

$$I_{\rho\rho}(z_1,\rho) = \frac{1}{2\pi} \int_{-\infty}^{0} du\, W'(|u|, z_1)\, \Im_{\rho\rho}(z_1,\rho)$$

(35)

An implicit dependence of $I_{\phi\phi}$ and $I_{\rho\rho}$ on z has been suppressed in (35).

For the exponential correlation function given in (19), an explicit expression for $I_{\phi\phi}$ can be obtained from Appendix C as,

$$
\begin{aligned}
I_{\phi\phi}(z_1,\rho) &= \frac{<|\xi|^2>}{\ell}\left\{ z_c(p,a) + \frac{\alpha_-(z_1)}{\sqrt{a(z_1)}}\, z_s(p,a) \right\} && z > z_1 \\
&= \frac{<|\xi|^2>}{\ell}\left\{ z_c(p,a) + \frac{\alpha_+(z_1)}{\sqrt{a(z_1)}}\, z_s(p,a) + \frac{[\alpha_+(z_1) - \alpha_+(z_1)]}{\sqrt{a(z_1)}}\, z_f(p,a) \right\} && z < z_1
\end{aligned}
\tag{36}
$$

where

$$
z_c(p,a) = \frac{2}{\left[p^2 + a(z_1)\right]^2}
$$

$$
z_s(p,a) = -\sqrt{a(z_1)}\ \frac{\left[3p^2 + a(z_1)\right]}{\left[p^3(p^2 + a(z_1)\right]}
$$

$$
\begin{aligned}
z_f(p,a) = {} & \frac{\sqrt{a(z_1)}}{p^3\left[p^2 + a(z_1)\right]} \exp[-p(z_1 - z)] \left\{ \left[\frac{3p^2 + a(z_1)}{p^2 + a(z_1)} + p(z_1 - z) \right] \cdot \right. \\
& \left. \left[\frac{p}{\sqrt{a(z_1)}} \sin[\sqrt{a(z_1)}(z_1 - z)] + \cos[\sqrt{a(z_1)}(z_1 - z)] \right] - \frac{p}{\sqrt{a(z_1)}} \sin[\sqrt{a(z_1)}(z_1 - z)] \right\}
\end{aligned}
\tag{37}
$$

The functions $a(z_1)$ are related to Green's function tensor and are defined in Appendix A. Similar expressions can be written for $I_{\rho\rho}$.

Eqs. (29) are the reduced form of the integral equations describing the second moment of the multiply scattered field. In the next section they will be put in a form suitable for solution by digital computer.

IV. SOLUTION OF THE INTEGRAL EQUATIONS

To put Eqs. (29) into a form suitable for digital computer programming, we transfer them to a set of linear algebraic equations which can be arranged into a linear matrix equation. Then matrix inversion techniques can be applied to solve the resultant matrix equation.

To transfer Eqs. (29) into a set of linear algebraic equations, the integration over ρ and over z_1 must be evaluated. Gaussian quadratures [6] will be employed here to evaluate the integrals over ρ.

As for integrals over z_1 we let

$$\int_{-\infty}^{0} dz_1 = \int_{-z_s}^{0} dz_1 + \int_{-\infty}^{-z_s} dz_1 \tag{38}$$

where z_s is the snow depth. Since the ground beneath the snow is homogeneous, the integration kernels vanish for any source point located below z_s. Accordingly, the second part of integration in (38) reduces to zero, and the lower limits of integration over z_1 in Eqs. (29) can be replaced by $z = z_s$.

The snow depth z_s is divided into (N-1) equal increments of dz each. Then by applying the trapezoidal rule, the integration over dz in (29) turns into a summation. The trapezoidal rule is applied here because through this rule the source point of the Green's function can be located ($z = z_1$) and the discontinuity in $a_{\rho z}$ and $a_{z\rho}$ at this point can be handled.

By introducing the vectors

$$\overline{E}_{na} = \begin{bmatrix} E_{11a}(z_n) \\ E_{22a}(z_n) \\ E_{33a}(z_n) \end{bmatrix}$$

$$\overline{E}^c_{na} = \begin{bmatrix} E^c_{11a}(z_n) \\ E^c_{22a}(z_n) \\ E^c_{22a}(z_n) \end{bmatrix}$$

(39)

Eqs. (29) can be written as

$$\overline{\overline{I}}\,\overline{E}_{na} + \overline{\overline{m}}_{nn}\left[\overline{E}_{na} + \overline{E}^c_{na}\right] = \sum_{j=1}^{N} \overline{\overline{M}}_{nj}\left[\overline{E}_{ja} + \overline{E}^c_{ja}\right]$$

(40)

where $\overline{\overline{I}}$ is the unit matrix and

$$\overline{\overline{m}}_{nn} = \begin{bmatrix} m_1(z_n) & m_2(z_n) & 0 \\ m_2(z_n) & m_1(z_n) & 0 \\ 0 & 0 & m_3(z_n) \end{bmatrix}$$

$$\overline{\overline{M}}_{nj} = \begin{bmatrix} M_{11}(z_n,z_j) & M_{12}(z_n,z_j) & f_{\rho z}(z_n,z_j) \\ M_{12}(z_n,z_j) & M_{11}(z_n,z_j) & f_{\rho z}(z_n,z_j) \\ f_{z\rho}(z_n,z_j) & f_{z\rho}(z_n,z_j) & f_{zz}(z_n,z_j) \end{bmatrix}$$

(41)

Eq. (40) represents a set of 3N algebraic equations. To solve these 3N equations we introduce new column matrices $\overline{E}_a$ and $\overline{E}^c_a$ having 3N components. The elements of these two new vectors are related to the elements of the field vectors given in Eq. (39) through the relations

$$E_{na}(i) = E_a(\,3[n-1]+i\,),$$

$$E^c_{na}(i) = E^c_a(\,3[n-1]+i\,)\,, \qquad \mathrm{i} = 1, 2, 3 \tag{42}$$

Accordingly, the 3N algebraic equations resulting from (40) can be arranged as follows:

$$\left[\,\bar{\bar{I}} - \bar{\bar{A}}\,\right]\bar{E}_a = \bar{\bar{A}}\,\bar{E}^c_a \tag{43}$$

where $\bar{\bar{A}}$ is a square matrix of order 3N. Its elements are related to the elements of the matrix given in (42) through the following relation :

$$m_{nn}(i,j)\,\delta_{mn} + M_{mn}(i,j) = A(\{3[n-1]+i\},\{3[m-1]+j\}), \qquad \mathrm{i}\,,\ \mathrm{j} = 1, 2,\ 3 \tag{44}$$

Eq. (43) is the matrix equation governing the second moment of the multiply scattered field. It may be solved by using either eigen value methods or a matrix inversion technique. Since the eigen values technique requires more computer resources (memory and computing time), only the matrix inversion techniques was considered in this study.

According to matrix inversion technique we premultiply Eq. (43) from both sides by the inverse of the matrix $[\bar{\bar{I}} - \bar{\bar{A}}]$ to write the multiply scattered field as

$$\bar{E}_a = \left[\bar{\bar{I}} - \bar{\bar{A}}\,\right]^{-1}\bar{\bar{A}}\,\bar{E}^c_a \tag{45}$$

The solution given in Eq. (45) is valid only when the determinant of the matrix $[\bar{\bar{I}} - \bar{\bar{A}}]$ has values other than zero. Numerical calculations using the developed FORTRAN program showed that the determinant of the matrix $[\bar{\bar{I}} - \bar{\bar{A}}]$ is controlled by two factors:

(i) the operating frequency (operating wavenumber k_o), and

(ii) the snow depth.

The determinant has a maximum value equal to unity. This value occurs when either the operating frequency or the snow depth is equal to zero. In both cases, there is no scattering occurring within the medium, and the elements of the matrix $\bar{\bar{A}}$ reduce to zero. Increasing either the operating frequency or the snow depth leads to an increase of the multiple scattering (increasing elements of $\bar{\bar{A}}$). The latter reduces the determinant until it reaches zero. In this case the operating frequency reaches a value equal to one of the medium resonance frequencies (eigen values). For frequencies higher than that frequency, Eq. (45) gives nonphysical values for the multiply scattered field. It may lead to a scattered intensity higher than the incident intensity or may give an intensity having negative values.

Based on the above discussion, the solution in (45) for the multiply scattered field is valid only when the determinant of the matrix $[\bar{\bar{I}} - \bar{\bar{A}}]$ has values greater than zero. This can be achieved by lowering either the operating frequency or decreasing the snow depth. The following table shows the maximum snow depth to which solution in Eq.(45) can be applied

Frequency (GHz)	37.0	50.0	85.0	91.6
snow depth (cm)	12.0	7.50	3.45	2.50

Table I

Table I is calculated for uniform snow, with snow density equal to 0.25 g/cm^3 and grain diameter equal to 0.7mm. Numerical calculations show that the values of the snow depth given in Table I can be increased by increasing the snow density or reducing the upper limit of integration over ρ (ρ_1 in Eq. (29)). For values of ρ_1 greater than k_o , total reflection occurs within the snow layer leading to a surface wave propagating along the layer interfaces.

The numerical limitations in solving the equation for the field second moments in the form discussed above were discovered rather late in the course of this work. Overcoming these restrictions will require significant modification in the FORTRAN program. Thus the examples to be discussed in Sec. V of the report will not cover the full range of conditions of interest in studying naturally occurring snowpacks.

The following paragraph will indicate some measures that can potentially be useful in extending the range of validity of the numerical calculations in future studies.

One method to increase the range of conditions for which a numerical solution is possible is to rearrange Eq. (40) as

$$(\bar{\bar{I}} + \bar{\bar{m}}_{nn})\bar{E}_{na} + \bar{\bar{m}}_{nn}\bar{E}^c_{na} = \sum_{j=1}^{N} \bar{\bar{M}}_{nj}[\,\bar{E}_{ja} + \bar{E}^c_{ja}] \tag{46}$$

By premultiplying (46) by the inverse of the matrix $(\bar{\bar{I}} + \bar{\bar{m}}_{nn})$, the equation

$$\bar{E}_{na} + (\bar{\bar{I}} + \bar{\bar{m}}_{nn})^{-1}\bar{\bar{m}}_{nn}\bar{E}^c_{na} = (\bar{\bar{I}} + \bar{\bar{m}}_{nn})^{-1}\sum_{j=1}^{N} \bar{\bar{M}}_{nj}[\,\bar{E}_{ja} + \bar{E}^c_{ja}] \tag{47}$$

is found. Then using Eq. (47) we obtain a matrix equation similar to Eq. (43). The determinant of the resultant matrix is greater than the determinant of the matrix $[\bar{\bar{I}} - \bar{\bar{A}}]$ of Eq. (43).

A further improvement for the solution can be achieved if in Eq. (40) we isolate the Green's function at the source point (n = j) in one side of the equation;

$$(\bar{\bar{I}} + \bar{\bar{m}}_{nn} - \bar{\bar{M}}_{nn})(\bar{E}_{na} + \bar{E}^{c}_{na}) = \bar{E}^{c}_{na} + \sum_{j \neq n}^{N} \bar{\bar{M}}_{nj}\left[\bar{E}_{ja} + \bar{E}^{c}_{ja}\right] \tag{48}$$

Eq. (48) may be rewritten as

$$[\bar{\bar{I}}\,\delta_{jn} - (\bar{\bar{I}} + \bar{\bar{m}}_{nn} - \bar{\bar{M}}_{nn})^{-1} \sum_{j \neq n}^{N} \bar{\bar{M}}_{nj}](\bar{E}_{ja} + \bar{E}^{c}_{ja}) = (\bar{\bar{I}} + \bar{\bar{m}}_{nn} - \bar{\bar{M}}_{nn})^{-1}\,\bar{E}^{c}_{na} \tag{49}$$

Eq. (49) is expected to lead to more stable matrix equation than Eq. (43). This is because the matrix on the right hand side of (49) reduces to the unit matrix for lower or higher values of the operating frequency or snow depth. The limit at lower values arises from the zero value of all $\bar{\bar{m}}_{nn}$ and $\bar{\bar{M}}_{nn}$ elements. The limit at higher values of the operating frequency or the snow depth arises because, the contribution of the source point $\bar{\bar{M}}_{nn}$ in (49) increases rapidly with increasing the operating frequency. On the other hand all other terms $\bar{\bar{M}}_{nj}$ decrease. Accordingly the second part of the matrix in the right hand side vanishes leading to a unit matrix to be inverted. Since programming Eq. (49) requires considerably more effort, it is recommended for another study.

V. NUMERICAL RESULTS AND DISCUSSION

The equations discussed in the previous sections were used to calculate the brightness temperature of snow at various frequencies and angles for particular snow conditions. These may be compared with the results obtained using the distorted Born approximation and reported in [3]. Reference [3] also shows ranges of measured brightness temperatures at various frequencies at a 50^o angle of incidence obtained from satellite borne radiometers. From the discussion in [3], a reasonable snow model describing the conditions at the satellite ground truth sites is snow at a temperature of -5^o C(268.15K), density $\rho = 0.25 g/cm^3$, and a grain diameter d = 0.7 mm. These values are adopted for most of the computations to be reported here together with the same atmospheric model and underlying soil conditions described in [3].

Figs. 2-4 show comparisons of the new calculations with the distorted Born approximation as a function of the angle of incidence, all for a radiometer at satellite altitude. The curve identifiers are the same in all of the figures. The initial letter (h or v) identifies the polarization (horizontal or vertical) while the second letter (m or s) identifies the theory : m=present theory with multiple scattering, s = distorted Born approximation (single scattering).

Figs.2-4 show the substantial effect of including the multiple scattering terms in the brightness temperature computations at high frequencies. These effects increases as the frequency increases from 37 GHz (Fig.2) to 50 GHz (Fig.3) to 91.6 GHz (Fig.4) as one would expect. Thus, for example, at an angle of incidence of 50^o and horizontal polarization, the inclusion of multiple scattering reduces the computed brightness temperature compared to the distorted Born approximation theory by 5.4K at 37 GHz to 12.1K at 50 GHz to 87.7K at 91.6 GHz. The corresponding decreases for vertical polarization are 4.2K at 37 GHz, 9.5K at 50 GHz, and 63.4K at 91.6 GHz.

Another perspective on these results is obtained by examining emissivities. Again choosing an observation angle of 50°, the emissivities corresponding to Figs. 2 - 4 are shown in Table II. It is clear that the distorted Born approximation emissivities reach a minimum between 37 and 91GHz and then increase with increasing frequency. This characteristic behavior of the distorted Born approximation calculation is not observed in measured data and, in fact was the principal reason for looking at more complete theories such as the subject of this report. On the other hand, with multiple scattering included, the emissivities decreases with increasing frequency.

TABLE II

Calculated emissivities of model snow pack at $\theta = 50^{o}$ ($\rho = 0.25 g/cm^3$, d=0.7 mm)

Frequency (GHz)	Horizontal Polarization		Vertical Polarization	
	Distorted Born	Multiple Scatter	Distorted Born	Multiple Scatter
37.0	0.8509	0.8439	0.9126	0.9054
50.0	0.8271	0.7725	0.8941	0.8399
91.6	0.8715	0.5352	0.9342	0.7315

Fig.5 shows computed brightness temperature as a function of snow depth at an angle of incidence of 50° for a frequency of 37 GHz. As discussed in Sec. IV, the present calculation method for multiple scattering is restricted to depths that are not too large. For the example in

Fig.5, the maximum snow depth at which the multiple scattering results should be considered trustworthy is about 12 cm. With this restriction in mind, it is interesting to compare the calculations in Fig.5 with satellite measurements. As discussed in [3], the reported range of brightness temperature values over the ground truth sites was 202 to 224K for horizontal polarization and 228 to 250K for vertical polarization for snow depths between 5 and 20 cm. The distorted Born approximation for horizontal polarization yields brightness temperature ranging from 234.4K to 225.4K in the snow depth range of 6 to 15 cm. This is on the high side. On the other hand, with multiple scattering included, computed brightness temperatures range from 229.1 to 208.4K in the 6 - 12 cm depth range (recall the earlier warning about depths larger than approximately 12 cm) and reach 224K at a depth of 7.5 cm. These values are seen to fall very nicely within the measured range. For vertical polarization, the distorted Born approximation calculations yield brightness temperature values ranging from 248.2K to 240.5K in the 5 to 15 cm snow depth range. While tending to be high, the calculations fall within the measured range. However, the new multiple scattering theory yields brightness temperatures in the 244.1K to 227.3K range for vertical polarization in 5 to 12 cm snow depth interval. This is comfortably within the measured range.

In [3], some discussion was devoted to the effects of non-uniformities such as a surface crust in the snowpack. At 37 GHz, non-uniformities in the snow structure were necessary in order for calculations with distorted Born approximation to match some of the low brightness temperatures that were measured for horizontal polarization. In particular, a model snowpack with a 1.5 mm surface crust with a density of 0.5 g/ cm^3 and a grain diameter d = 1 mm was assumed to cover an otherwise uniform snowpack with the parameters used above. When the multiple scattering theory is applied to these conditions, the brightness temperature for a snow depth of 10 cm was found to be 195K for horizontal polarization. Extrapolating possible effects to larger snow depths (recall the present limit to about 12 cm so that a direct computation is not possible) indicates that the calculated brightness temperature in the range 170K to 180K may be

found at horizontal polarization at 37 GHz. This is near the lower bound of measurements made over Siberia for large snow depths and is much better than the lowest value of 202K found with distorted Born approximation under the same conditions. If lower bulk snow densities were to be used together with a very cold and dry atmosphere, the distorted Born approximation does lead to brightness temperature with horizontal polarization that are closer to the lower limit of the measurements over Siberia as was shown in [3]. However, the calculated vertically polarized brightness temperatures are still too high (lowest value achieved is 214K with the reduced snow density and 238K with $\rho = 0.5$ g/cm^3 and the standard atmospheric conditions) compared to the measured low of 196K. With the multiple scatter model, even using a snow density of 0.25 g/cm^3 yields a vertically polarized brightness temperature of 208K for a snow depth of 10 cm. Extrapolating to larger snow depths and lower snow densities indicates that values near 196K can be reached when multiple scattering is included.

New information at even higher frequencies has become available since the publication of [3]. This is the data obtained by SSM/I instrument at 85.5 GHz at an angle of 53.1^o. Brightness temperature measurements over snow by the SSM/I at this frequency are often in the 150 - 180K range for horizontal polarization although, depending on snow conditions, values in the 200 to 240K range are also found. For vertical polarization, brightness temperatures as low as 160 K are sometimes found, but more typically are in the 230 to 255K range. According to Fig.4 (at the slightly displaced frequency of 91.6 GHz), the calculated horizontally polarized brightness temperature at an angle of 53^o is 162K when multiple scattering is included versus 244K for the distorted Born approximation if the snow density is 0.25 g/cm^3 . Thus, the multiple scattering model result fits comfortably within the measured range while the distorted Born approximation value is much too high. Computations were also performed for snow densities of 0.3, 0.4 and 0.5 g/cm^3 at 91.6 GHz. For horizontal polarization, calculated brightness temperatures at an angle of 53^o and using the multiple scattering theory increased to 177K at 0.3g/ cm^3 to 209K at 0.4 g/cm^3 to 224K at 0.5 g/ cm^3 showing that a reasonable range of snow densities can account for the

range of brightness temperatures measured by SSM/I. In contrast, the distorted Born approximation yields horizontally polarized brightness temperatures in the small range 236 - 243K for the same snow density range and actually decrease with the increasing snow density. These are too high. For vertical polarization, multiple scattering theory yields brightness temperatures of 196, 206, 231, and 246K for snow densities of 0.25, 0.3, 0.4 and 0.5 g/cm^3 respectively. This is nicely within the range of values measured by the SSM/I. On the other hand, the calculated distorted Born approximation brightness temperatures are in the very small range 255 - 257K for vertical polarization as the snow density range from 0.25 g/cm^3 to 0.5 g/cm^3. Clearly, the distorted Born approximation calculations can not explain the measurements.

VI. CONCLUSIONS AND RECOMMENDATIONS

The computations discussed in Sec. V show that a very great improvement in agreement between the calculated and measured snow brightness temperatures is achieved when using the extension of the distorted Born approximation (multiple scattering) theory as compared to the distorted Born approximation itself at frequencies above 30 GHz. This agreement is obtained without the arbitrary, ad-hoc parameter adjustments (often euphemistically called effective parameters) that are made in radiative transfer models and relies strictly on random media parameters that can be measured.

It is particularly gratifying that calculations at 91.6 GHz (near the SSM/I 85.5 GHz frequency and coinciding with the SSM/T-2 and SSMIS 91.6 GHz channels) using reasonable snow parameters yielded brightness temperatures within ranges measured by the SSM/I for both horizontal and vertical polarizations. These values were much lower than those obtained by use of the distorted Born approximation. The latter were unreasonably high at 91.6 GHz.

Certain numerical difficulties (discussed in Sec.IV) were discovered which prevented the computation of brightness temperatures with multiple scattering theory over the full range of snow depths, densities and radiometer frequencies of practical interest. Contract funds for exploring possible corrective actions were depleted when the problem came to light. However, possible strategies for overcoming this computational problem were discussed, and it is recommended that a follow on study be undertaken to resolve the problems. If these problems are resolved, the theory may then be applied to the study of multi - year sea ice with and without snow cover. On the basis of the results obtained to date, one may expect to obtain the first quantitative explanations of the high frequency measurements obtained by the SSM/I over

multi - year ice as well as measurements to be obtained by future instruments such as the SSMIS at even higher frequencies (e.g., 150 GHz).

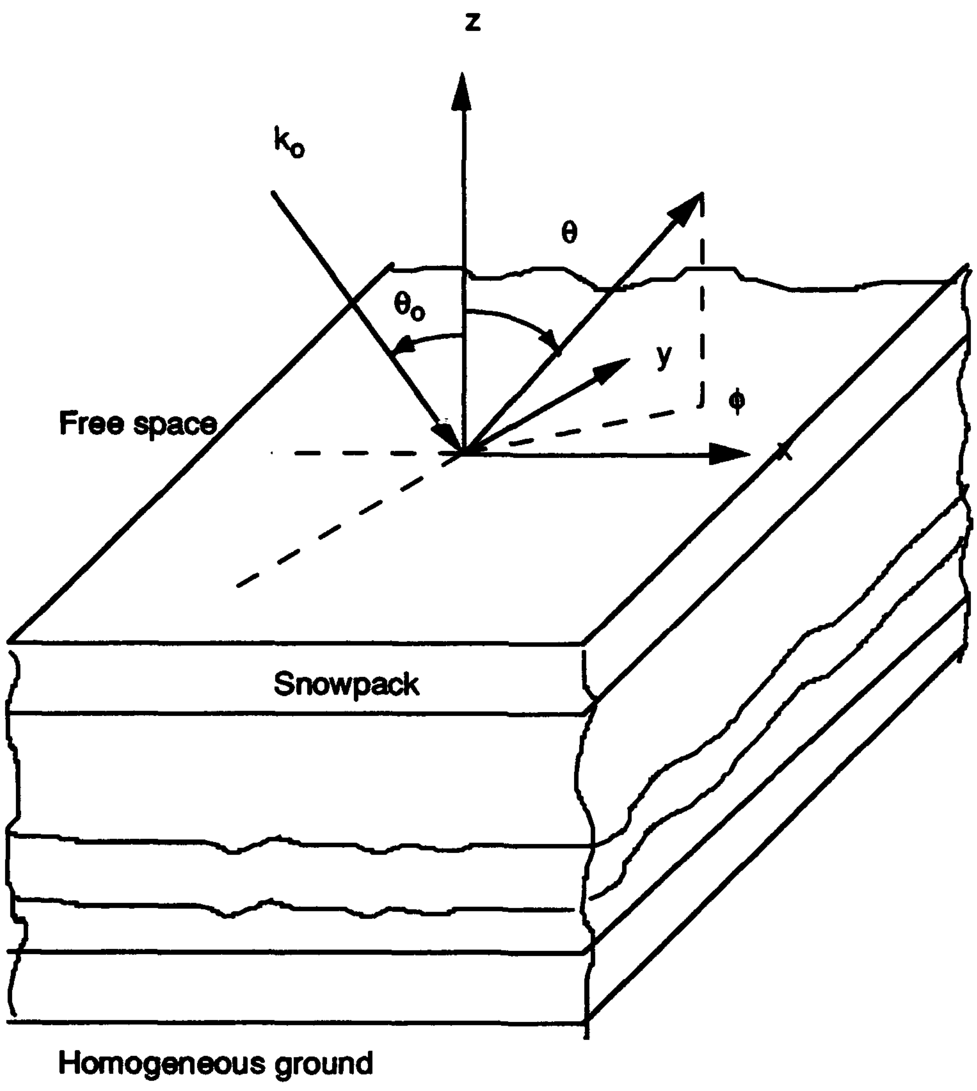

Fig.1 Geometry for brightness temperature computation.

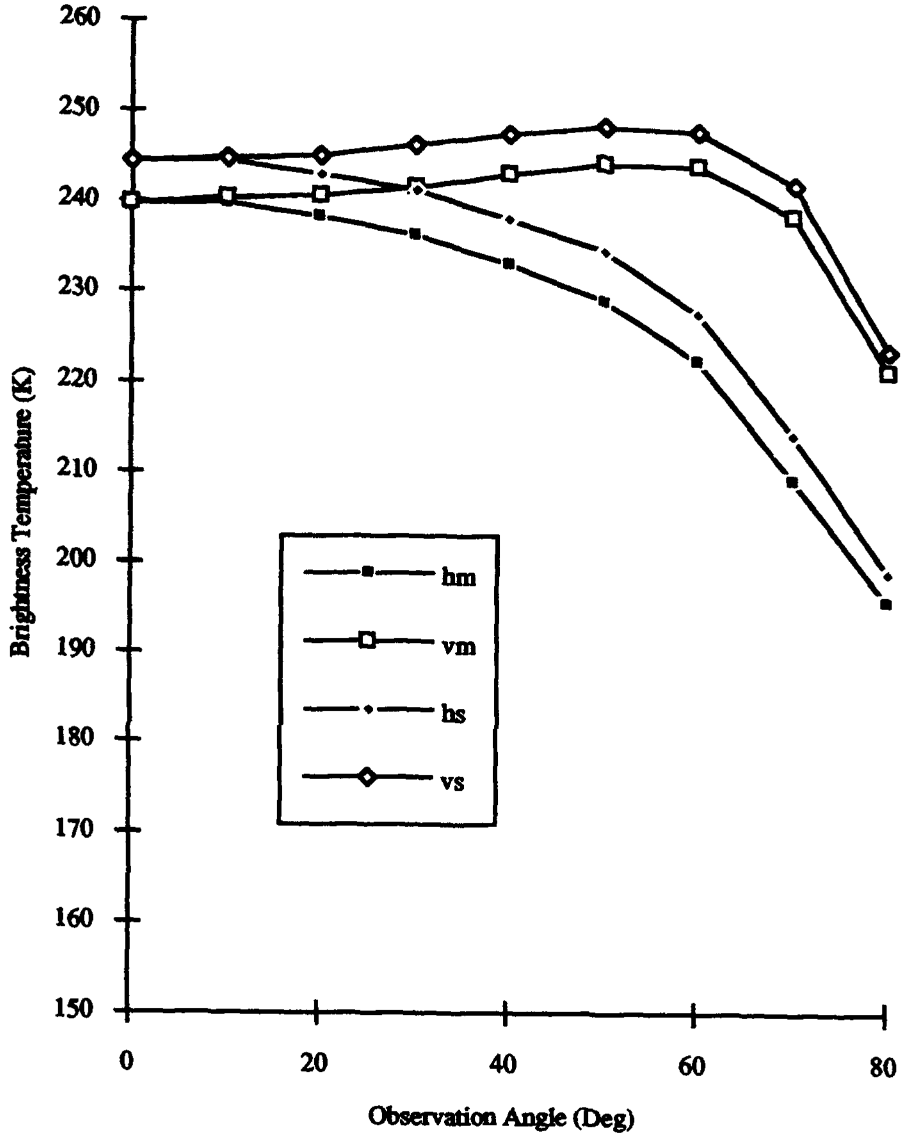

Fig. 2 Computed brightness temperatures of uniform dry snow at 37 GHz and depth of 6 cm.

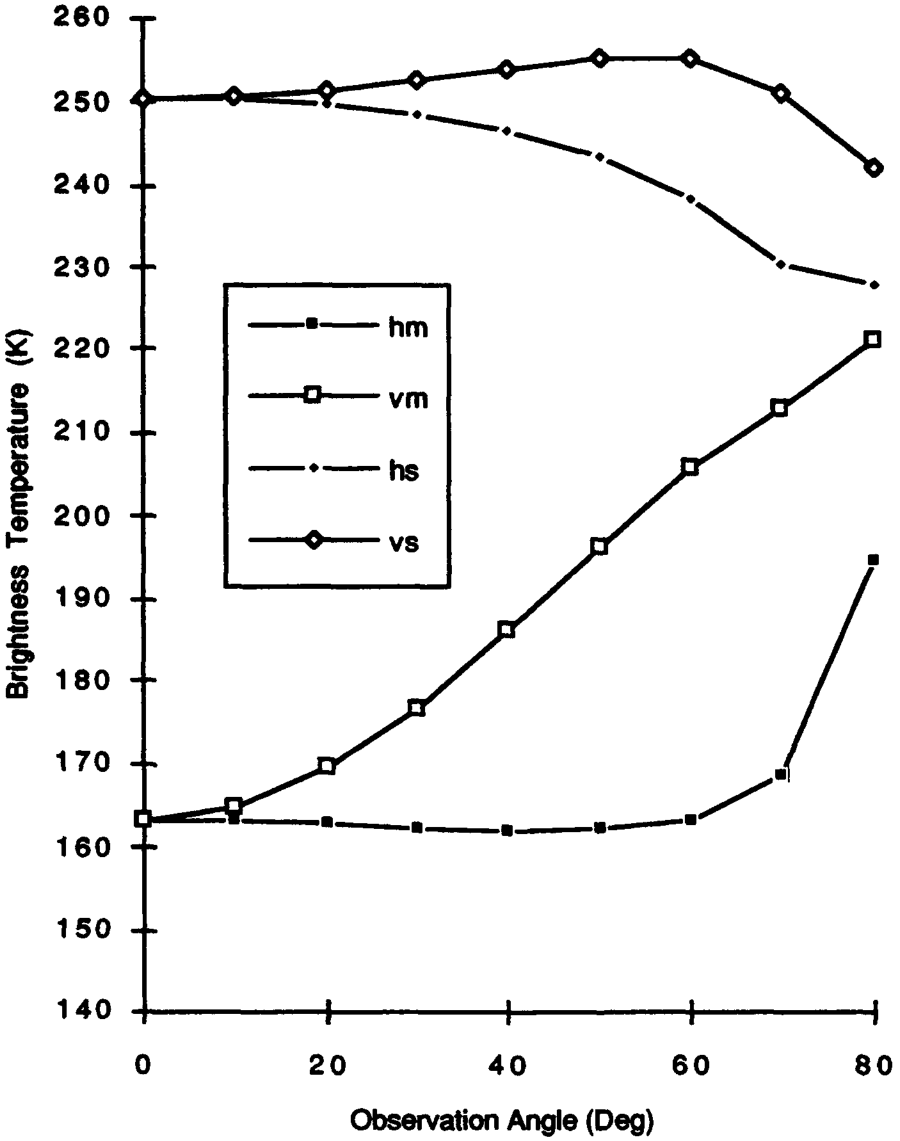

Fig. 3 Computed brightness temperatures of uniform dry snow at 50 GHz and depth of 6 cm.

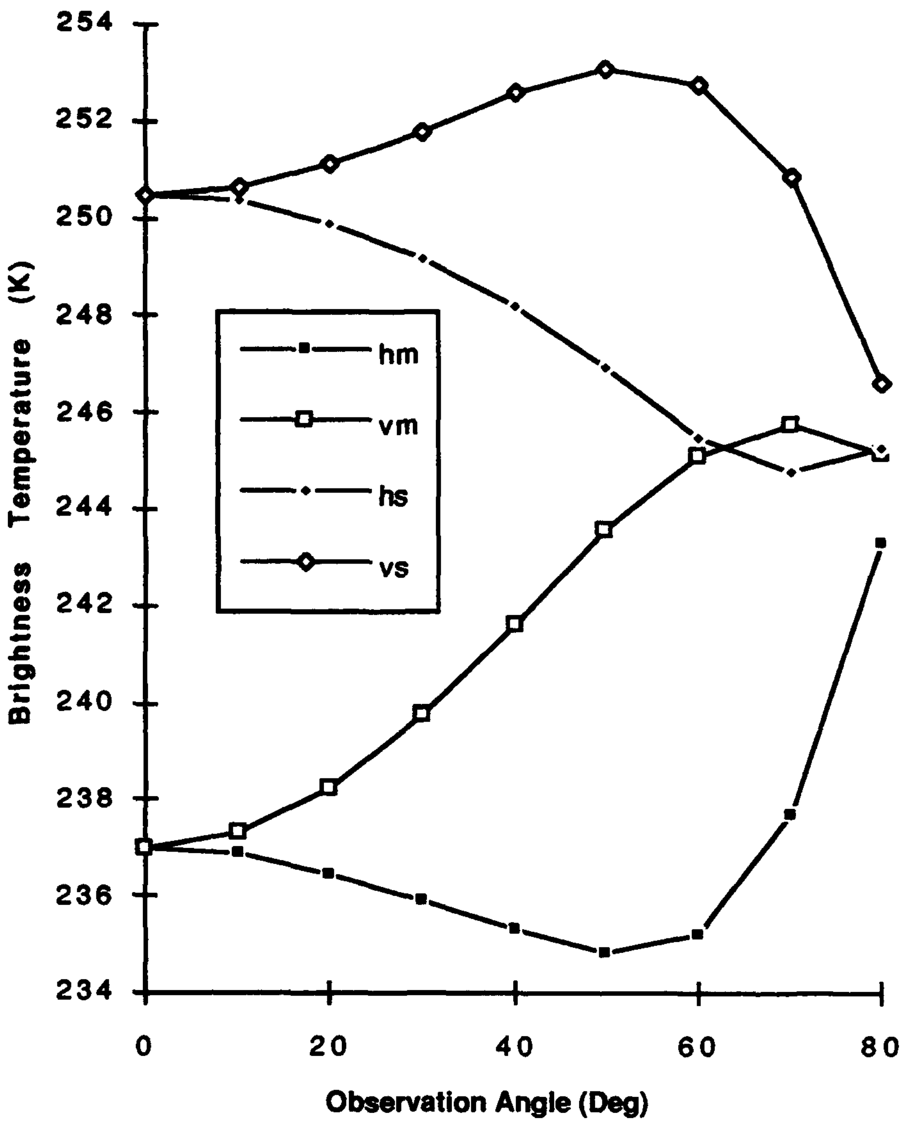

Fig. 4 Computed brightness temperatures of uniform dry snow at 91.6 GHz and depth of 2.5 cm.

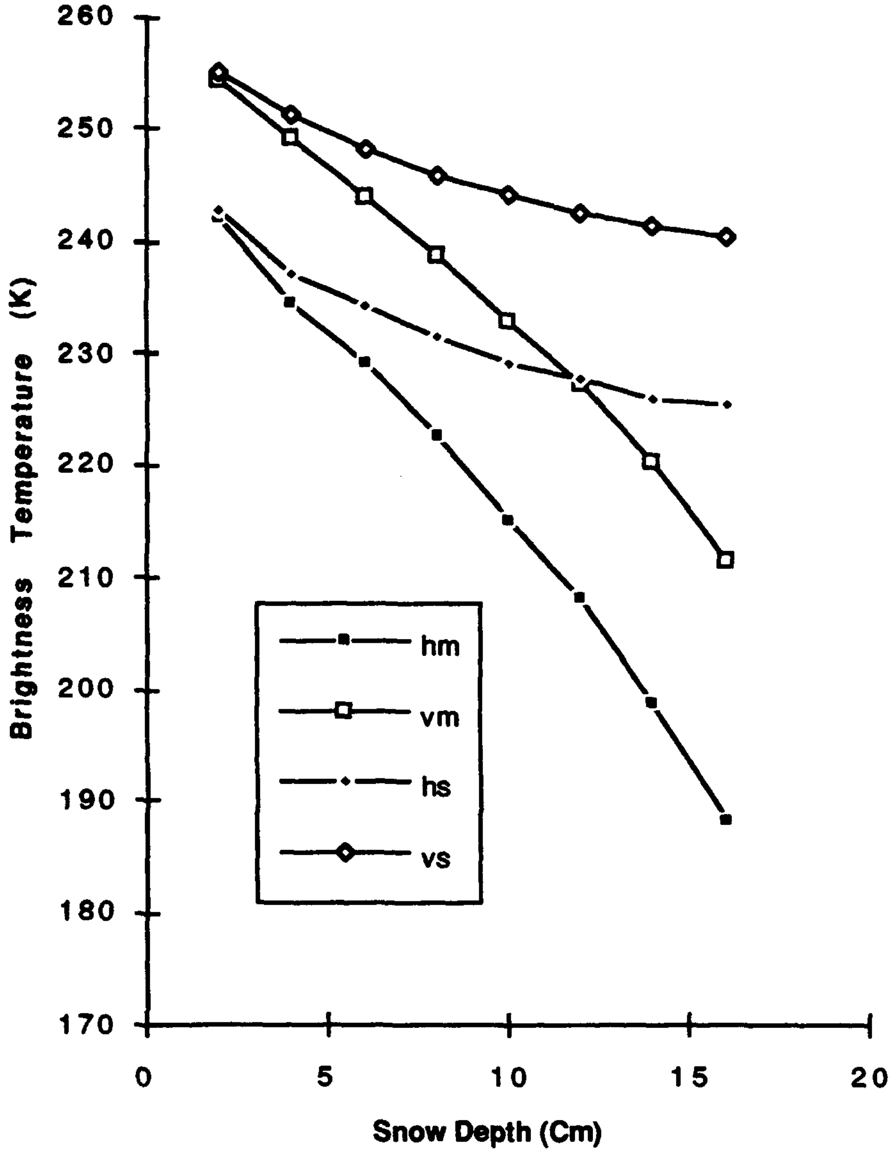

Fig.5 Computed brightness temperatures of uniform dry snow at 37 GHz and 50^{o} angle of incidence

APPENDIX A

THE DYADIC GREEN'S FUNCTION

As seen in Sec.II and Sec.III, the dyadic Green's function elements are required to determine the random field second moment. Since the medium horizontal dimensions extend to infinity, it is convenient to express the dyadic Green's function tensor in terms of a two dimensional Fourier transform,

$$\overline{\overline{\Gamma}}(\bar{r},\bar{r}') = \frac{1}{2\pi}\int_{-\infty}^{\infty} dk_x \int_{-\infty}^{\infty} dk_y\, \overline{\overline{a}}(z,z',k_x,k_y)\exp\{\, j[k_x(x-x') + k_y(y-y')]\}$$

(A-1)

where

$$\overline{\overline{a}}(z,z',k_x,k_y) = a_{\rho\rho}\,\hat{\rho}\hat{\rho} + a_{\rho z}\,\hat{\rho}\hat{z} + a_{\phi\phi}\,\hat{\phi}\hat{\phi} + a_{z\rho}\,\hat{z}\hat{\rho} + a_{zz}\,\hat{z}\hat{z}$$

(A-2)

Explicit formulations for the Green's function tensor elements in terms of the medium dielectric properties have been derived in [1]. In this Appendix only the formulations required for the present study will be summarized.

The first element that will be considered is $a_{\phi\phi}$ which has the following formulation [1];

$$\begin{aligned} a_{\phi\phi} &= \exp\Big[\int_{z'}^{z}\alpha_+(z'')dz''\Big] / [\,\alpha_-(z') - \alpha_+(z')\,] && \text{if } z > z' \\ &= \exp\Big[-\int_{z}^{z'}\alpha_-(z'')dz''\Big] / [\,\alpha_-(z') - \alpha_+(z')\,] && \text{if } z < z' \end{aligned}$$

(A-3)

The α 's in (A-3) are governed by the differential equation

$$d\alpha_{\pm} / dz + \alpha_{\pm}^2 + a(z) = 0 \tag{A-4}$$

with

$$a(z) = k_o^2 K_o(z) - \rho^2, \qquad \rho^2 = k_x{}^2 + k_y{}^2 \tag{A-5}$$

Eq. (A-4) is subjected to the boundary conditions

$$\alpha_+(0) = j\sqrt{k_o{}^2 - \rho^2}$$
$$\alpha_-(-\infty) = -j\sqrt{a(-\infty)} \tag{A-6}$$

At a point of dielectric constant discontinuity $(z = -d)$, α 's satisfy

$$\alpha_{\pm}(-d) \Big[_{-d-0}^{-d+0} = 0 \tag{A-7}$$

As for $a_{\rho\rho}$ in (A-2), it can be written as

$$a_{\rho\rho} = a(z')\left[k_o^2 K_o(z')\right]^{-1} \exp\left[\int_{z'}^{z} \beta_+(z'')\,dz''\right] / [\beta_-(z') - \beta_+(z')] \qquad \text{if } z > z'$$
$$= a(z')\left[k_o^2 K_o(z')\right]^{-1} \exp\left[-\int_{z}^{z'} \beta_-(z'')\,dz''\right] / [\beta_-(z') - \beta_+(z')] \qquad \text{if } z < z' \tag{A-8}$$

The β 's in (A-8) are governed by the differential equation

$$d\beta_{\pm} / dz + \beta_{\pm}^2 - b(z)\,\beta_{\pm} + a(z) = 0 \tag{A-9}$$

with

$$b(z) = \rho^2 \frac{dK_o(z)}{dz} / [a(z) K_o(z)]$$

(A-10)

Eq. (A-9) is subjected to the boundary conditions

$$\beta_+(0) = \frac{j\, a(0)}{K_o(0) \sqrt{k_o^2 - \rho^2}}$$

$$\beta_-(-\infty) = -j \sqrt{a(-\infty)}$$

(A-11)

At a point of dielectric constant discontinuity $(z = -d)$ the β 's satisfy the condition

$$(K_o / a)\, \beta_\pm \Big|_{-d-0}^{-d+0} = 0$$

(A-12)

The other elements of Green's function tensor $(a_{\rho z}, a_{z\rho}, a_{zz})$ can be related to $a_{\rho\rho}$ through the relation

$$a_{ij} = f_{ij}(z,z')\, a_{\rho\rho}(z,z') - \left[1 / k_o^2 K_o\right] \delta(z - z')\, \delta_{iz}$$

(A-13)

The factor $f_{ij}(z,z')$ in (A-13) varies from one Green's function component to another. Also for the same Green's function component, the value of this factor may vary depending on the relative locations of the field z and source z' points to each other. Explicit expressions for $a_{\rho z}, a_{z\rho}$, and a_{zz} are given in [1].

For a field point located in the upper half space $(z > 0)$, the Green's function components in (A-1) and (A-2) can be written as

$$\overline{\overline{a}}(z,z',k_x,k_y) = \overline{\overline{A}}\,(z',k_x,k_y)\exp(j\,k_z z) \tag{A-15}$$

APPENDIX B

THE AUXILIARY PROPAGATION FUNCTIONS

A complete description for the Green's tensor elements requires explicit expressions for auxiliary propagation functions α's and β's ($\pm$ is dropped for convenience). Also it requires the evaluation of an exponential raised to a power equal to the integral of these auxiliary functions.

To obtain an explicit expression for α we write the differential equation (A-4) describing α as

$$\frac{d\alpha(z)}{a(z)+\alpha^2(z)} = dz \tag{B-1}$$

and assume that over the interval of interest, the dielectric properties do not vary so much that the dielectric constant may by replaced by its mean value. Then integrating both sides of (B-1) we obtain

$$\alpha(z) = \sqrt{a}\,\tan\left[\sqrt{a}\,(c-z)\right] \tag{B-2}$$

where a is the mean value of $a(z)$ in the interval. In (B-2) c is a constant which can be determined by writing (B-2) as

$$\alpha(z) = \sqrt{a}\,\tan\left[\sqrt{a}\,(z_1-z)+\sqrt{a}\,(c-z_1)\right] \tag{B-3}$$

If we let $\alpha = \alpha_1$ at $z = z_1$, we can write α from (B-3) as

$$\alpha(z) = \frac{\sqrt{a}\,\tan[\sqrt{a}(z_1 - z)] + \alpha_1}{1 - \frac{\alpha_1}{\sqrt{a}}\tan[\sqrt{a}(z_1 - z)]}$$

(B-4)

To evaluate the exponential in (A-3) we use (B-2) to write

$$\int_{z_1}^{z_2} \alpha\, dz = -\int_{z_1}^{z_2} \sqrt{a}\,\tan[\sqrt{a}(z - c)]\, dz = \ln\left(\frac{\cos[\sqrt{a}(z_2 - c)]}{\cos[\sqrt{a}(z_1 - c)]}\right)$$

(B-5)

where ln is the natural logarithm. From (B-5), the exponential in (A-4) can be written as

$$\exp\left(\int_{z_1}^{z_2} \alpha\, dz\right) = \frac{\cos[\sqrt{a}(z_2 - z_1) + \sqrt{a}(c - z_1)]}{\cos[\sqrt{a}(c - z_1)]}$$

(B-6)

With some mathematical manipulations (B-6) can be reduced to

$$\exp\left(\int_{z_1}^{z_2} \alpha\, dz\right) = \cos[\sqrt{a}(z_2 - z_1)] + \frac{\alpha_1}{\sqrt{a}}\sin[\sqrt{a}(z_2 - z_1)]$$

(B-7)

To obtain explicit expression for the auxiliary function β first we reduce the differential equation (A-9) governing β to a form similar to the differential equation (A - 4) governing α. This can be achieved through scaling β as

$$\beta = \lambda \beta'$$

(B-8)

Then substituting (B-8) in (A-9) to get

$$\lambda\, d\beta' / dz + \beta'^2 \lambda^2 + a(z) + \beta'\, d\lambda / dz - b(z)\, \beta'\, \lambda = 0$$

(B-9)

In (B-9) letting

$$d\lambda / dz = b(z)\, \lambda$$

(B-10)

and dividing the resultant over λ^2 the differential equation governing β' reduces

$$d\beta' / du + \beta'^2 + \nu = 0$$

(B-11)

Which is similar to Eq. (A-4) describing α. In (B-11) we have,

$$u = \lambda z$$

$$\nu = a / \lambda^2$$

(B-12)

By analogy to (B-4), and (B-7) we can write

$$\beta' = \frac{\sqrt{\nu'}\ \tan[\sqrt{\nu'}\ \lambda(z_1 - z) + \beta'_1}{1 - \frac{\beta'_1}{\sqrt{\nu'}} \tan[\sqrt{\nu'}\ \lambda(z_1 - z)]}$$

(B-13)

and;

$$\exp[\int_{z_1}^{z_2} \beta\, dz\,] = \cos[\sqrt{\nu}\,\lambda(z_2 - z_1)] + \frac{\beta'_1}{\sqrt{\nu}} \sin[\sqrt{\nu}\,\lambda(z_2 - z_1)]$$

(B-14)

To obtain the explicit expression of λ and ν we substitute for b form (A-10) into (B-9) to get

$$d\lambda / \lambda = \frac{\rho^2}{K}\ \frac{1}{k_o^2 K - \rho^2}\, dK$$

(B-15)

Integrating both sides of (B-15) leads to;

$$\lambda = \frac{k_o^2 K - \rho^2}{k_o^2 K} = \frac{a(z)}{k_o^2 K}$$

(B-16)

Then by substituting (B-16) into (B-12) we get

$$\nu = \frac{k_o^4 K^2}{a(z)} = \frac{k_o^4 K^2}{k_o^2 K - \rho^2}$$

(B-17)

APPENDIX C

ANALYTIC EVALUATION OF THE INTEGRALS IN EQS. (23) and (35)

In this Appendix, the integrals $I_{\phi\phi}$ and $I_{\rho\rho}$ in Eqs. (23) and (35) will be evaluated analytically. Since there is analogy between α and β as has been discussed in Appendix B, only the evaluation of the integral $I_{\phi\phi}$ will be considered in detail. Then by analogy the integral $I_{\rho\rho}$ will be evaluated.

To evaluate the integral $I_{\phi\phi}$, from (B-7) we recall

$$\exp\left(\int_{z_1}^{z_2} \alpha \, dz\right) = \cos[\sqrt{a}(z_2 - z_1)] + \frac{\alpha_1}{\sqrt{a}} \sin[\sqrt{a}(z_2 - z_1)] \tag{C-1}$$

Also we write the power spectrum for the exponential correlation function (Eq.20) as

$$W(|u|,\rho) = <|\xi|^2> \frac{2\pi}{\ell} f(|u|,\rho) \tag{C-2}$$

where

$$\begin{aligned} f(|u|,\rho) &= p^{-3}[1 + p|u|]\exp(-p|u|) \\ p &= [1 + \ell^2 \rho^2]^{1/2} / \ell \end{aligned} \tag{C-3}$$

Then we introduce the integrals

$$z_c(p,a) = \int_{-\infty}^{0} du\, f(|u|,\rho) \cos(\sqrt{a}\, u) = \frac{2}{[p^2 + a]^2}$$
$$z_s(p,a) = \int_{-\infty}^{0} du\, f(|u|,\rho) \sin(\sqrt{a}\, u) = -\frac{\sqrt{a}}{p^3 [\, p^2 + a\,]^2} \{ 3p^3 + a \}$$

(C-4)

For $z > z_1$ we can write $I_{\phi\phi}$ as

$$I_{\phi\phi} = \frac{<|\xi|^2>}{\ell} \left[z_c(p,a) + \frac{\alpha_-(z_1)}{\sqrt{a}} z_s(p,a) \right]$$

(C-5)

For $z < z_1$ we can write $I_{\phi\phi}$ as

$$I_{\phi\phi} = \frac{<|\xi|^2>}{\ell} \left[z_c(p,a) + \frac{\alpha_-(z_1)}{\sqrt{a}} z_s(p,a) + \frac{\alpha_+(z_1) - \alpha_-(z_1)}{\sqrt{a}} \int_{z-z_1}^{0} du \sin(\sqrt{a}u) \right]$$

(C-6)

By evaluating the integral in (C-6) we can write $I_{\phi\phi}$ as

$$I_{\phi\phi} = \frac{<|\xi|^2>}{\ell} \left[z_c(p,a) + \frac{\alpha_+(z_1)}{\sqrt{a}} z_s(p,a) + \frac{\alpha_+(z_1) - \alpha_-(z_1)}{\sqrt{a}} z_f(p.a) \right]$$

(C-7)

where

$$z_f(p,a) = \frac{\sqrt{a}}{p^3 [\, p^2 + a\,]} \exp(-p|z - z_1|) \Big\{ \Big[\frac{[\,3p^2 + a\,]}{[\, p^2 + a \;]} + p(z_1 - z) \Big] .$$
$$\Big[\frac{p}{\sqrt{a}} \sin\{\sqrt{a}(z_1 - z)\} + \cos\{\sqrt{a}(z_1 - z)\} \Big] - \frac{p}{\sqrt{a}} \sin\{\sqrt{a}(z_1 - z)\} \Big\}$$

(C-8)

By analogy to (C-5) and (C-7) we can write the integral I_{pp} as

$$I_{pp} = \frac{<|\xi|^2>}{\ell} \, [\, z_c(p,\nu) + \frac{\beta_-(z_1)}{\lambda\sqrt{\nu}} \, z_s(p,\nu)\,]$$

(C-9)

For $z > z_1$, and

$$I_{pp} = \frac{<|\xi|^2>}{\ell} \, [\, z_c(p,\nu) + \frac{\beta_+(z_1)}{\lambda\sqrt{\nu}} \, z_s(p,\nu) + \frac{\beta_+(z_1) - \beta_-(z_1)}{\lambda\sqrt{\nu}} \, z_f(p.\nu)\,]$$

(C-10)

For $z < z_1$ where,

$$z_f(p,\nu) = \frac{\sqrt{\nu}}{p^3[\,p^2+\nu\,]} \exp(-p|z-z_1|) \Big\{\Big[\frac{[\,3p^2+\nu\,]}{[\,p^2+\nu\ \ ]} + p(z_1 - z) \Big]$$

$$\Big[\frac{p}{\sqrt{\nu}} \sin\{\sqrt{\nu}(z_1 - z)\} + \cos\{\sqrt{\nu}(z_1 - z)\} \Big] - \frac{p}{\sqrt{\nu}} \sin\{\sqrt{\nu}(z_1 - z)\} \Big\}$$

(C-11)

All parameters in (C-9), (C-10) and (C-11) are given in (B-6), (B-7), (B-16), and (B-17).

REFRENCES

1- Stogryn, A.," Investigation of extensions to the distorted Born approximation in strong fluctuation theory," Contract No. N00014-87-0784, Report 9316 (October 1988), prepared for the Office of Naval Research by Aerojet ElectroSystems Company.

2- Stogryn, A.," Strong fluctuation theory equations for electric field second moments in anisotropy media," *IEEE Transaction on Antennas and Propagation,* vol.38, no.7, pp. 1099-1101, 1990.

3- Stogryn, A., "A study of the microwave brightness temperature of snow from the point of view of strong fluctuation theory," *IEEE Transaction on. Geoscience and Remote Sensing*, vol. GE-24, pp. 220-231, 1986.

4- Stogryn, A.," A study of the microwave brightness temperature of sea ice ," Contract No. N00014-85-C-0765 (December 1986), prepared for the Office of Naval Research by Aerojet ElectroSystems Company.

5- Stogryn, A.," The bilocal approximation for the electric field in strong fluctuation theory," *IEEE Transaction on Antennas and Propagation,* vol. AP-31, pp. 985-986, 1983.

6- Abramowitz, M, and I.A. Stegun, *Handbook of Mathematical Functions,* Dover Publications, Inc., New York, 1972.